TUPR48

FERMILAB-POSTER-24-0039-AD

Sextupole Misalignment and Defect Identification and Remediation in IOTA

J. Wieland, A. Romanov, Fermilab

Nonlinear integrable optics studies at the integrable optics test accelerator (IOTA) require accurate control of chromaticity and closed orbit.

IOTA has 6 symmetric sextupole families. During operations during the last electron run undesirable effects on the closed orbit were observed

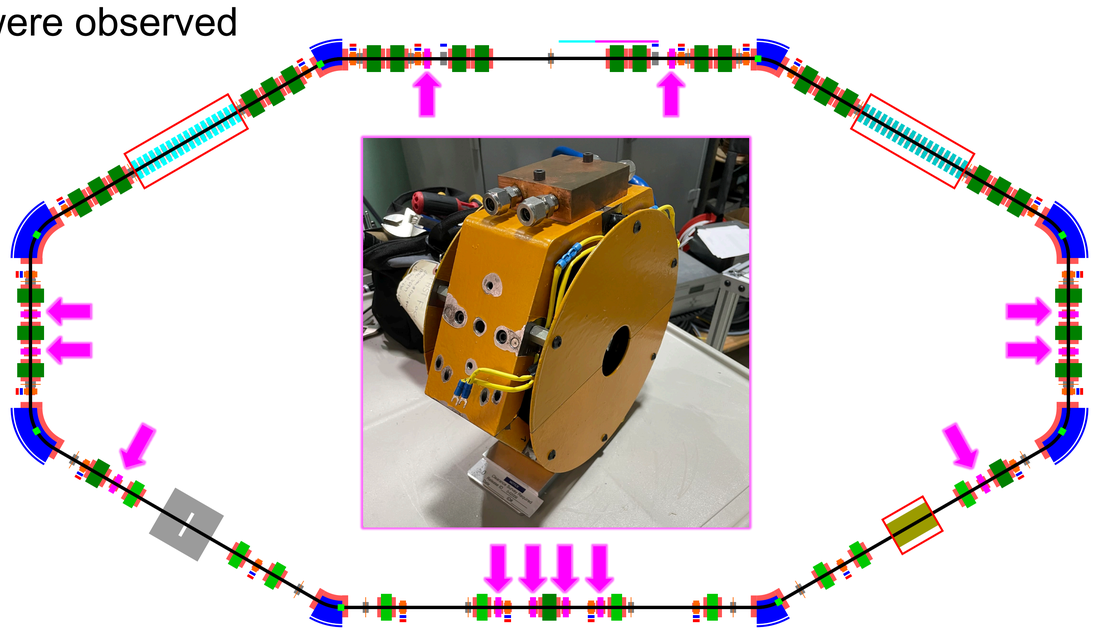

Test Stand Measurements

After the run was completed, a sextupole which exhibited a large dipole term in the beam-based measurements was removed from the ring. Magnetic field maps with a 3-D hall probe were performed. Scans were performed with the Fermilab technical division test stand and the FAST test stand for benchmarking.

Right: Field map illustration and multipole decomposition for sextuple at +2A excitation. Multipole terms are centered by zeroing quadrupole term.

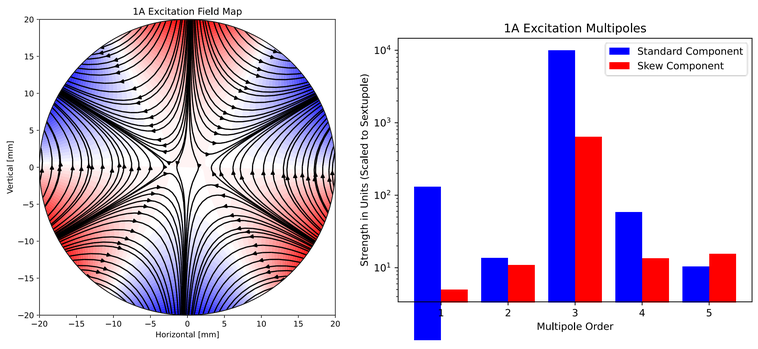

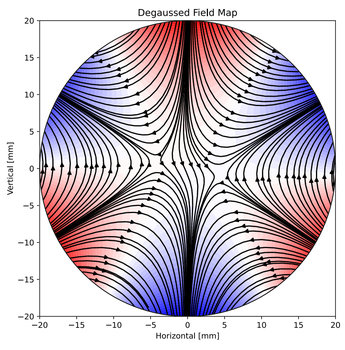

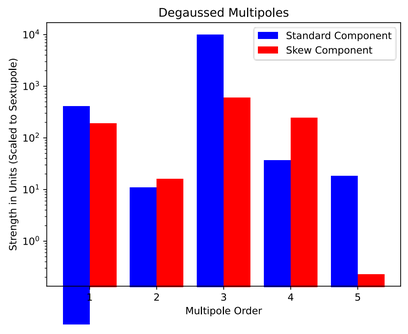

Left: Field map illustration and multipole decomposition for sextuple after degaussing. Central field is at noise floor for hall probe used for measurements.

Initial evaluation was to compare to beam based results. The sextupole was then degaussed, with good results on residual field. Dipole term continued to appear after degaussing when excited, indicating hysteresis was not dominant effect.

Simulation Studies

Simulation studies in Mermaid excluded pole displacement, yoke misalignment, and missing coil turns of reasonable magnitude as the source of measured dipole term.

Scan Config	Bx [mT]	By [mT]
1A Excitation	-0.01	-0.28
Degaussed	2e-3	-5e-3
Negative Hysteresis	-0.13	0.10
Positive Hysteresis	0.16	-0.11

Above: Summary of Central fields for plotted field scans.

Beam Based Measurements

The closed orbit response to sextupole excitations for different orbit bumps was measured. Assuming a thin dipole kick, the fields were calculated. The sextupole geometry was then reconstructed from the measured fields. Vertical fields were small and error dominated, so horizontal orbit effects were used.

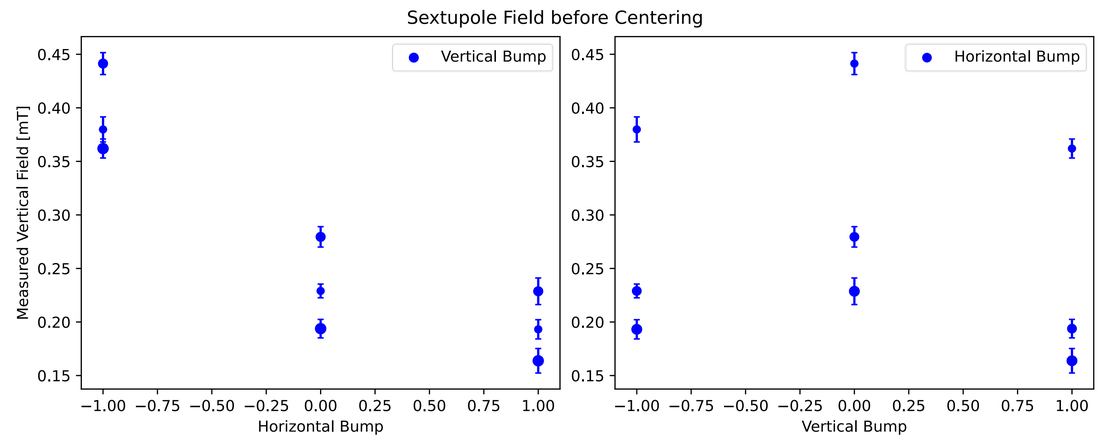

Above: Calculated field from closed orbit deviations. Marker size is proportional to orthogonal bump magnitude.

Right: Fit results for sextupole before and after in situ mechanical alignment, expression above table

$$B_y = b_3((x + x_o)^2 - (y + y_o)^2) + b_1$$

Fitted Value	Uncentered	Centered
X offset [mm]	0.87	0.21
Y offset [mm]	-0.12	0.03
b1 [mT]	0.23	0.28

Residual Magnetization Evaluation

The degaussing effectively cleared the hysteresis in the magnet, but dipole terms appeared at excitation. Scans of residual magnetization after large positive and negative excitation were performed to evaluate geometry.

Right: Field map illustration and multipole decomposition for residual magnetization scan after excitation at +2A. Poles demonstrate asymmetric residual magnetization.

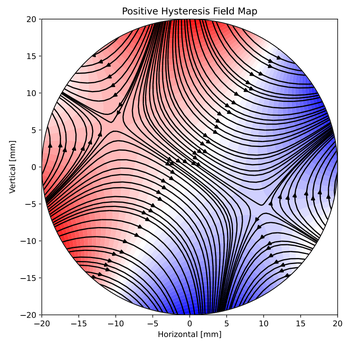

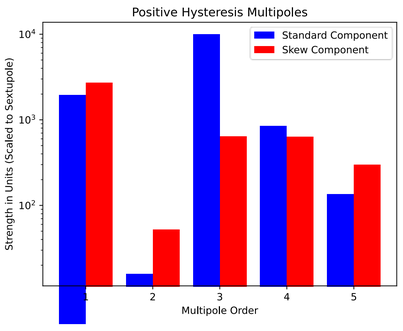

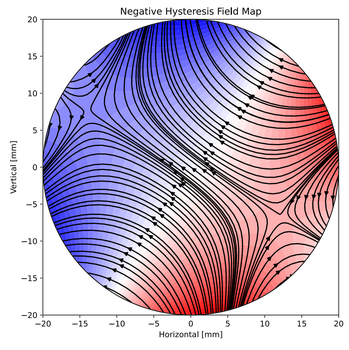

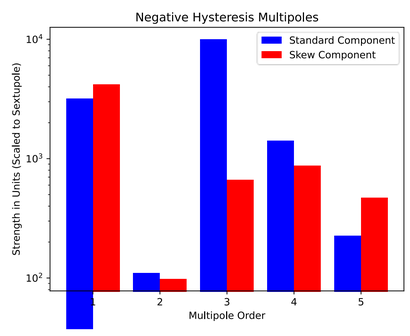

Left: Field map illustration and multipole decomposition for residual magnetization scan after excitation at -2A. Geometry is reversed as expected.

Below: Calculated field magnitude on reference magnitude after centering

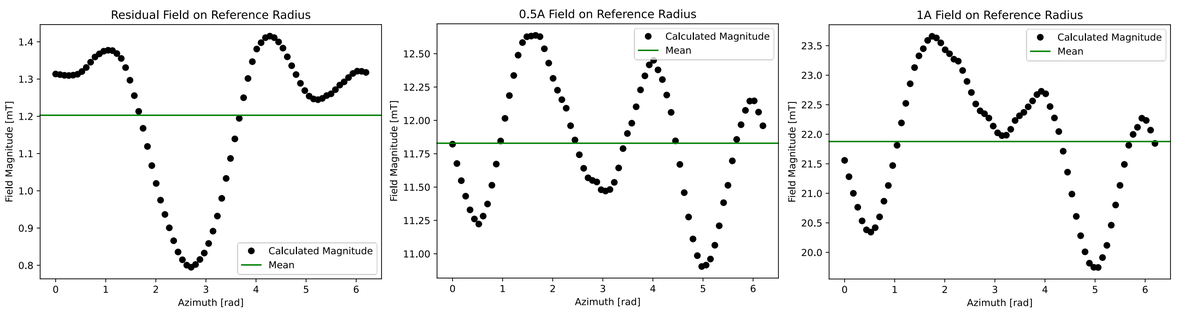

Field magnitude on reference radius shows undesirable shift. We suspect inconsistent magnetic qualities of the pole material. Next steps for this magnet family will be removing the poles and evaluating replacements for proper magnetization.

Fermi National Accelerator Laboratory

This manuscript has been authored by Fermi Research Alliance, LLC under Contract No. DE-AC02-07CH11359 with the U.S. Department of Energy, Office of Science, Office of High Energy Physics